fibers

MDPI

Article

Enhancement Experiment on Cementitious Activity of Copper-Mine Tailings in a Geopolymer System

Lin Yu [1,2,†], Zhen Zhang [1,†], Xiao Huang [1,†], Binquan Jiao [1,2,*] and Dongwei Li [1,*]

1 State Key Laboratory for Coal Mine Disaster Dynamics and Control, Chongqing University, Chongqing 400044, China; 15808085585@139.com (L.Y.); zz15866741253@163.com (Z.Z.); shawwong@126.com (X.H.)

2 City College of Science and Technology, Chongqing University, Chongqing 400044, China

* Correspondence: j.binquan@cqu.edu.cn (B.J.); litonwei@cqu.edu.cn (D.L.)

† These authors contributed equally to the work.

Received: 21 September 2017; Accepted: 14 December 2017; Published: 15 December 2017

Abstract: Copper-mine tailings are the residual products after the extraction of precious copper metal from copper ores, and their storage can create numerous environmental problems. Many researchers have used copper-mine tailings for the preparation of geopolymers. This paper studies the enhancement of the cementitious activity of copper-mine tailings in geopolymer systems. First, copper-mine tailings are activated through mechanical grinding activation. Then, the mechanically activated copper-mine tailings are further processed through thermal activation and alkaline-roasting activation. The cementitious activity index of copper-mine tailings is characterized through the degree of leaching concentration of Si and Al. It was observed that the Si and Al leaching concentration of mechanically activated tailings was increased by 26.03% and 93.33%, respectively. The concentration of Si and Al was increased by 54.19% and 119.92%, respectively. For alkaline-roasting activation, roasting time, temperature and the mass ratio of copper-mine tailings to NaOH (C/N ratio) were evaluated through orthogonal tests, and the best condition for activation was 120 min at 600 °C with a C/N ratio of 5:1. In this study, scanning electron microscopy (SEM), X-ray diffraction (XRD) and infra-red (IR) analysis show that mechanical, thermal and alkaline-roasting activation could be used to improve the cementitious activity index of copper-mine tailings.

Keywords: copper-mine tailings; mechanical activation; thermal activation; alkaline-roasting activation; alkali leaching

1. Introduction

Concrete is widely used as a construction material with annual production of more than 10 billion tons worldwide [1]. Ordinary Portland Cement (OPC) is the main constituent of concrete. One ton of cement is produced at a cost of 1.5 tons of raw material and 0.7 tons of carbon dioxide being emitted into the atmosphere [2]. Cement production not only consumes a large amount of natural resources but also emits carbon dioxide which causes atmospheric pollution. The cement industry is responsible for 7% of the total emissions of carbon dioxide across the world [3–5]. China is the largest cement producer and consumer across the world, and is also suffering from air pollution [6]. Therefore, it is important to find alternatives to cement. Geopolymers are a new type of binders that have cementitious characteristics upon alkaline activation. They have many advantages compared to OPC, because of better performance and cost-effective production [7,8]. Geopolymers are formed through geopolymerization processes in which (a) solid aluminosilicates are activated by alkali solution to generate aluminate and silicate tetrahedral monomers; (b) the monomers form silica–alumina oligomers which subsequently form inorganic polymeric material; (c) these inorganic polymeric materials condense into hardened geopolymers [8].

Geopolymers are used as building materials and also for the solidification of heavy metals. In addition to fly ash and metakaolin, various aluminosilicate minerals, clays, solid wastes, and their mixtures have also been used to synthesize geopolymers [9]. Glukhovsky and Krivenko used alkali-activated metallurgical slag in construction materials in the 1950s [10]. The first concept of geopolymers and geopolymerization was proposed by Davidovits in 1972 [11]. Further progression in geopolymers was summarized by Davidovits and Orlinski in the 1980s [12–14]. In contrast, Wastiels et al. [15] described alkaline activation of fly ash-based geopolymers in the 1990s. Rahier et al. [16–20] synthesized aluminosilicate glasses at low temperatures and carried out studies on metakaolin-based geopolymers. Several raw materials containing Si and Al have been used for alkaline activation but very few studies have been conducted on the geopolymerization of copper-mine tailings [21–24]. To date, Zhang et al. and Ahmari et al. [25,26] have investigated the effect of different factors such as activators (type and concentrations) and curing temperature using copper-mine tailings as alkali-activated binders. They concluded that copper-mine tailings can be used as raw materials for the preparation of geopolymers. However, there are some limitations such as the effect of high curing temperature and concentration of alkali solution on geopolymers. Hence, some modifications are required to overcome these limitations.

The main objective of this study is to investigate the effects of three conditions—(a) mechanical grinding, (b) thermal activation, and (c) alkaline roasting activation—on the improvement of the cementitious activity index of copper-mine tailings in geopolymer systems. The tailings were activated at five different temperatures for various time intervals after mechanical grinding. Orthogonal tests were designed to achieve the optimal set of experimental parameters: mass ratio of copper-mine tailings to NaOH (C/N ratio), roasting time and roasting temperature. The cementitious activity of copper-mine tailings was identified by the leaching analysis. Scanning electron microscopy (SEM), infra-red (IR) and X-ray diffraction (XRD) analysis were used to investigate the particle morphology and mineral composition of copper-mine tailings.

2. Materials and Methods

2.1. Materials

The source material used in this experiment was copper-mine tailings processed through flotation. The samples were collected from Yangla copper industry, Yunnan, China. The chemical composition of the copper-mine tailings is reported in Table 1. Silica and alumina with a substantial amount of iron and calcium can be seen. The particle size and cumulative distribution were analyzed by LSPSDA (Mastersizer 2000, Malverng, Malvern, UK), as shown in Figure 1. It can be seen that the particles with a diameter of less than 100 μm account for 60% of the mine tailings. Morphological characteristics tested by SEM (NOVA400, FEI, Hillsboro, FL, America) were presented in Figure 2. Results showed that copper-mine tailings were unevenly distributed with irregular shapes; large particles have smooth and angular surfaces, and small particles are adsorbed on to the surface of the large particles. XRD analysis was performed with a D/max-RB diffractometer using CuK_a radiation (40 kV and 100 mA), at 4°/min ranging from 10° to 70°. The main crystalline materials in the copper mine tailings were quartz (SiO_2), albite ($NaAlSi_3O_8$), Chlorite $(Mg, Al)_6(SiAl)_4O_{10}(OH)_8$ and dolomite $(CaMg(CO_3)_2)$ (Figure 3). Fourier transform infra-red (FITR) spectroscopy analysis was performed by a FTIR system (Nicolet5DXC, Thermo Nicolet Corporation, Madison, WI, America) in the range of 400–4000 cm^{-1}.

Table 1. Chemical composition (wt %) of copper-mine tailings.

SiO_2	Al_2O_3	Fe_2O_3	CaO	K_2O	Na_2O	MgO	SO_3
58.5	13.3	10.7	5.4	4.0	2.8	1.9	0.6

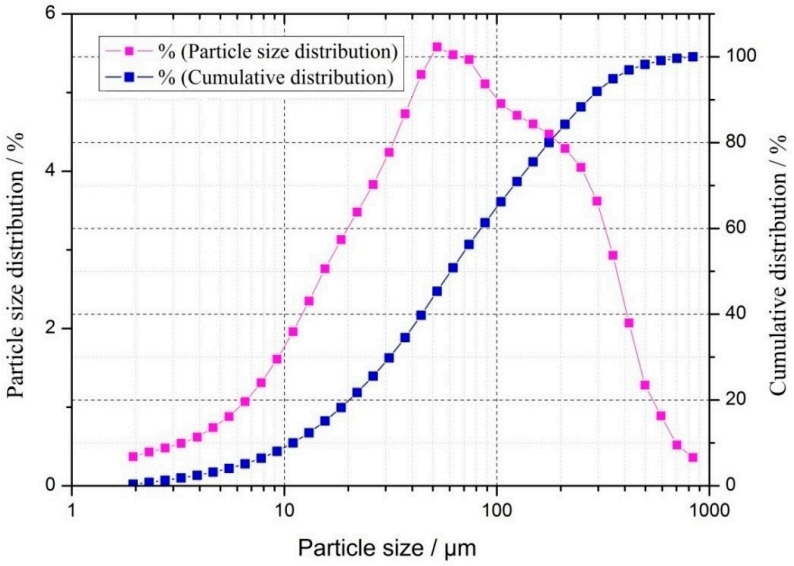

Figure 1. Particle size and cumulative size distribution of raw copper-mine tailings.

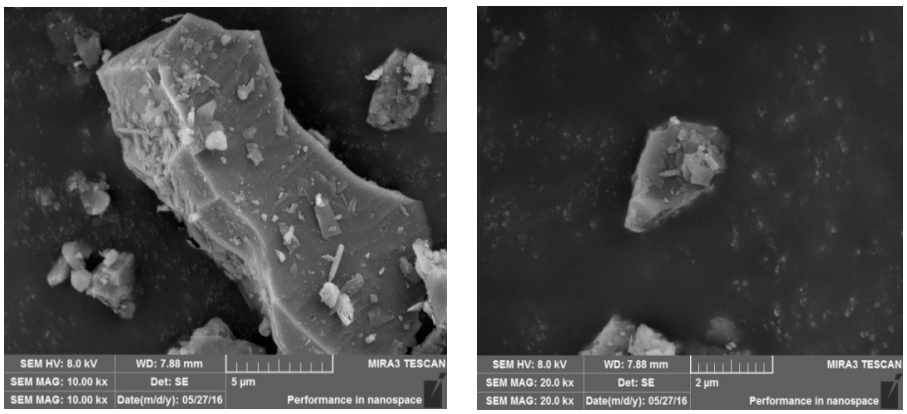

(**a**) 10,000× (**b**) 20,000×

Figure 2. Scanning electron microscope (SEM) images of raw copper-mine tailings' powder (10,000 (**a**) and 20,000 (**b**) magnification).

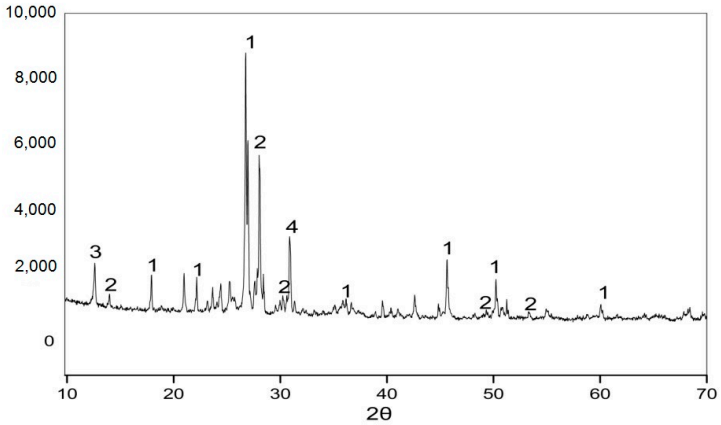

Figure 3. X-ray diffraction (XRD) pattern of raw copper-mine tailings' powder (1 quartz, 2 albite, 3 chlorite, 4 dolomite).

2.2. Methods

2.2.1. Mechanical Activation of Copper-Mine Tailings

A laboratory ball mill (SN-500, Rongsheng, Tangshan, China) was used to improve the activity index of copper-mine tailings, and the grinding media was steel balls (powder: steel balls, 1:10). One kilogram of copper mine tailings was activated each time. The grinding time and mass ratio of the ball are two important factors that influence the mechanical grinding of copper-mine tailings. In the current study, samples were ground for different periods (Table 2) at 200 rpm.

Table 2. The experimental layout of the mechanical grinding of copper-mine tailings.

No.	Grinding Time (h)
M1	1.0
M1.5	1.5
M2	2.0
M2.5	2.5
M3	3.0
M3.5	3.5
M4	4.0
M4.5	4.5

2.2.2. Thermal Activation of Copper-Mine Tailings

Thermo-gravimetric–differential scanning calorimetry (TG–DSC) (STA 449C, Netzsch, Selb, Germany) was used to examine the thermal characteristics of the samples. Temperature and activation time are two important factors which influence the thermal activation of copper-mine tailings. Therefore, experiments were carried out at 10 °C to 1200 °C in atmospheric conditions for 4 time periods (60 min, 90 min, 120 min, 150 min). Table 3 summarizes the thermal activation parameters of copper-mine tailings.

Table 3. Thermal activation parameters of copper-mine tailings.

Sample Name (TM)	Calcination Temperature (°C)	Calcination Time (min)
TM 1	400	60
TM 2	400	90
TM 3	400	120
TM 4	400	150
TM 5	500	60
TM 6	500	90
TM 7	500	120
TM 8	500	150
TM 9	600	60
TM 10	600	90
TM 11	600	120
TM 12	600	150
TM 13	700	60
TM 14	700	90
TM 15	700	120
TM 16	700	150
TM 17	800	60
TM 18	800	90
TM 19	800	120
TM 20	800	150

2.2.3. Alkaline-Roasting Activating of Copper-Mine Tailings (ARMT)

Three fundamental factors affecting the cementitious activity of copper-mine tailings such as roasting time, temperature and C/N ratio were evaluated through orthogonal tests. Firstly, the copper-mine tailings were mixed with a NaOH solution. The mixture was oven dried for 24 h. The copper-mine tailings and NaOH mixtures were roasted in a muffle furnace for different periods and temperatures (Table 4). These tailings were activated by alkaline roasting and named as ARMT samples. The parameters with their respective levels and orthogonal experimental layout are presented in Tables 4 and 5, respectively.

Table 4. Parameters with their levels used in alkaline-roasting activation of copper-mine tailings (ARMT) samples.

Levels	Factors		
	A	B	C
	Roasting Time (min)	Roasting Temperature (°C)	C/N Ratio
1	60	550	5:1
2	90	600	7.5:1
3	120	650	10:1

Table 5. Orthogonal experimental layout of ARMT samples.

No.	A	B	C	Result
ARMT1	1 (60 min)	1 (550 °C)	1 (5:1)	y_1
ARMT2	1	2 (600 °C)	2 (7.5:1)	y_2
ARMT3	1	3 (650 °C)	3 (10:1)	y_3
ARMT4	2 (90 min)	1	2	y_4
ARMT5	2	2	3	y_5
ARMT6	2	3	1	y_6
ARMT7	3 (120 min)	1	3	y_7
ARMT8	3	2	1	y_8
ARMT9	3	3	2	y_9

2.2.4. Leaching Test

Leaching analysis was performed to study the effects of different activation methods on the dissolution of silica and alumina species from copper-mine tailings. The first step of geopolymerization processes is the dissolution of solid aluminosilicate materials into aluminates and silicate tetrahedral monomers in the presence of alkaline solution. The leaching test can also be used to measure the cementitious activity of copper tailings. A sample of 1 g copper-mine tailings was immersed in 100 mL NaOH solution (1 M) in a polyethylene beaker and sealed after stirring. After curing (7 days) in a standard curing box at 20 ± 1 °C, the solution was filtrated and diluted 100 times. The concentration of Al and Si in the solution was analyzed by using an inductively coupled plasma optical-emission spectrometer (ICP-OES) (Model ICAP 6300, Thermo Fisher Scientific, Waltham, MA, USA). Table 6 shows the mixture ratios for ARMT samples in alkaline-leaching experiments.

Table 6. Mixture ratios of ARMT samples and NaOH solution used in alkaline-leaching experiments.

Sample	Sample Quantity (g)	Quantity of NaOH in the Solution (g)
ARMT1, ARMT6, ARMT8	1.200	3.800
ARMT2, ARMT4, ARMT9	1.133	3.867
ARMT3, ARMT5, ARMT7	1.100	3.900

3. Results and Discussion

3.1. Mechanical Activation of Copper-Mine Tailings

3.1.1. Leaching Test

Si and Al concentrations from leaching experiments are given in Figure 4. It can be seen that the maximum leaching concentration of Si is 47.02 μg/mL (M3) and Al is 18.98 μg/mL (M4.5) after mechanical grinding. A significant increase in the leaching concentrations of Si and Al was obtained compared to the raw copper-mine tailings and the values were 26.03% and 93.33%, respectively. This phenomenon was also consistent with previous results reported by Wang et al. [27].

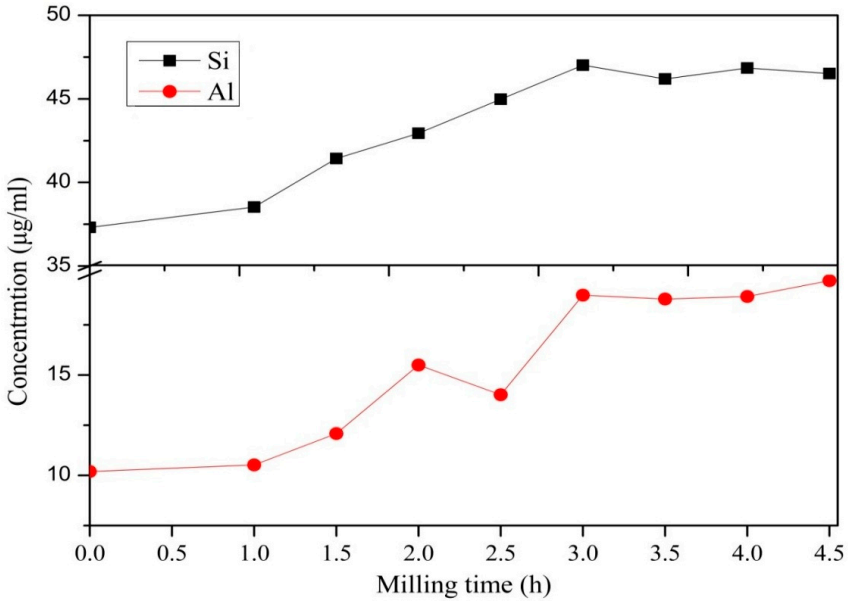

Figure 4. Si and Al leaching concentrations after mechanical activation of copper-mine tailings.

3.1.2. Effect of Mechanical Activation on Particle Size Distribution

Figure 5 shows the cumulative particle size distribution of milled copper-mine tailings against time. The curves slowly shift to the left side with the increase in grinding time. In contrast, after 3 h, curves begin to shift to the right side. This illustrates that the particle size of copper-mine tailings was gradually decreased with the increase in grinding time up to 3 h and then increased. Moreover, the particles of the M3 sample of less than 10 μm in size increased by 20% compared to the original sample (increasing by as much as 31.45%). Meanwhile, particles of less than 44.00 μm in size increased by as much as 89.63%. Particle sizes D50 and D90 at different grinding times for the copper-mine tailings are illustrated in Figure 6. It can be seen that particle sizes D50 and D90 are rapidly decreased with the increase in grinding time. After 3 h of grinding, the particle sizes D50 and D90 reach their minimum sizes of 16.98 μm and 44.53 μm, respectively. This indicates that, after 3 h, continuous grinding causes a gradual increase in particle size, which suggests that particles start to bond together. This agrees with the previous results in literature [28]. Therefore, 3 h can be considered as the optimal mechanical grinding time under these conditions.

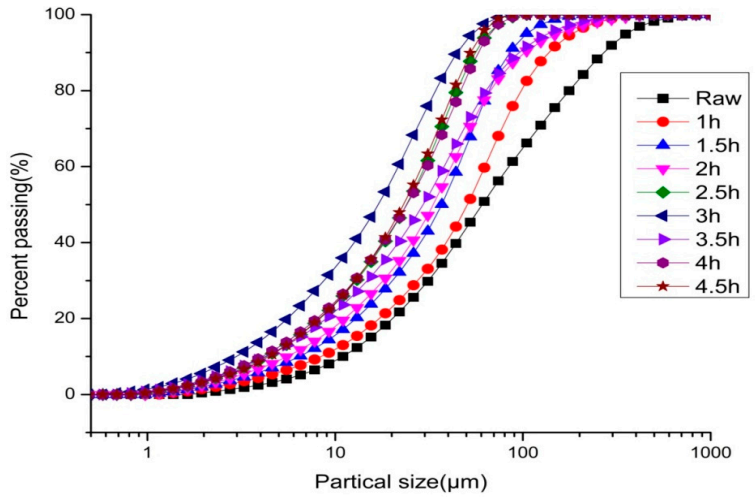

Figure 5. The effect of grinding on the particle sizes of copper-mine tailings at different time intervals.

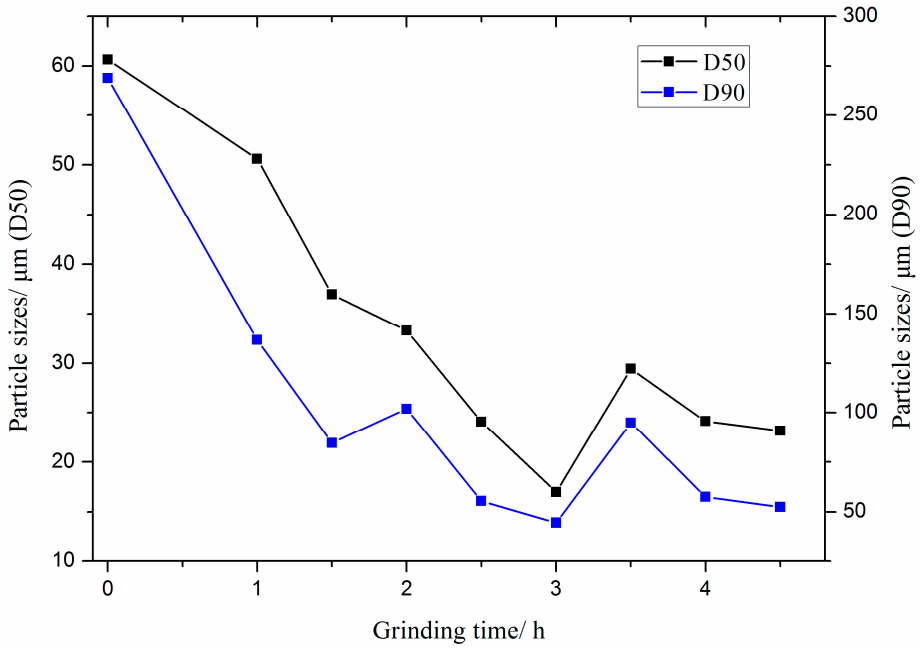

Figure 6. Variations of particle sizes (D50 and D90) of copper-mine tailings after grinding.

3.1.3. Particle Morphology and Mineral Composition

Figure 7 shows the SEM images of the sample M3. Si and Al ions were easily leached down due to the presence of smaller particles (as a result of mechanical grinding). Figure 8 shows the XRD patterns of raw and treated copper-mine tailings (sample M3). No significant difference was observed among diffraction peaks, which indicates that no new phases are formed. Moreover, the effect of mechanical activation can be seen by the formation of less intensive peaks of crystalline silica; the intensity of the albite diffraction peak is increased after mechanical activation. Si and Al are leached more easily as a result of grain refinement. It can be seen from Figure 9 that the Si(Al^{IV})-O-Si asymmetric stretching band is reduced from 1005.41 cm^{-1} to 1004.99 cm^{-1} and Si-O bend vibrations (533.30 cm^{-1} and 462.43 cm^{-1}) are reduced to 530.84 cm^{-1} and 461.52 cm^{-1}, respectively. This indicates that the polymerization degree of $[SiO_4]^{4-}$ and $[AlO_6]^{9-}$ ions of copper-mine tailings are reduced. This is because the Si-O and Si(Al^{IV})-O-Si bonds of copper-mine tailings are gradually broken during mechanical activation. Improvement was thus observed in the cementitious activity index of copper-mine tailings.

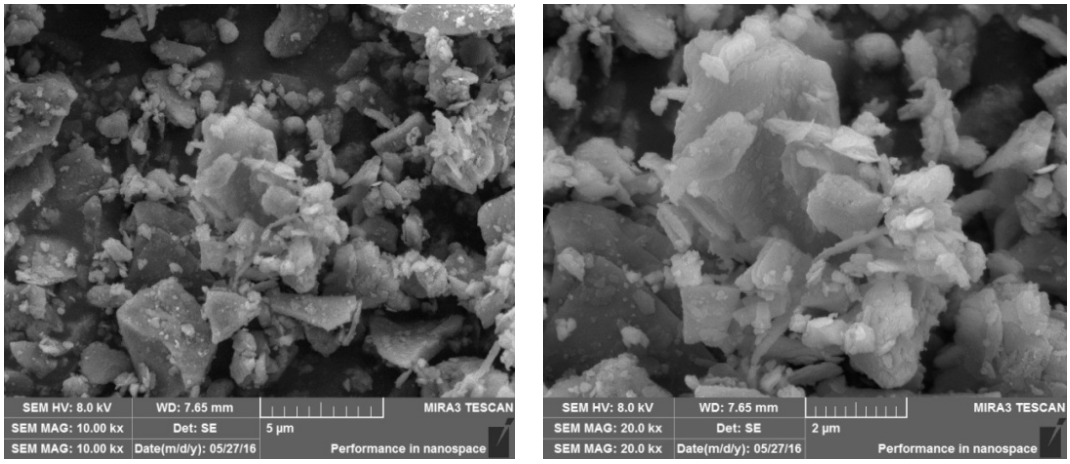

(**a**) 10,000× (**b**) 20,000×

Figure 7. SEM images of activated sample M3 (after 3 h of grinding) (10,000 (**a**) and 20,000 (**b**) magnification).

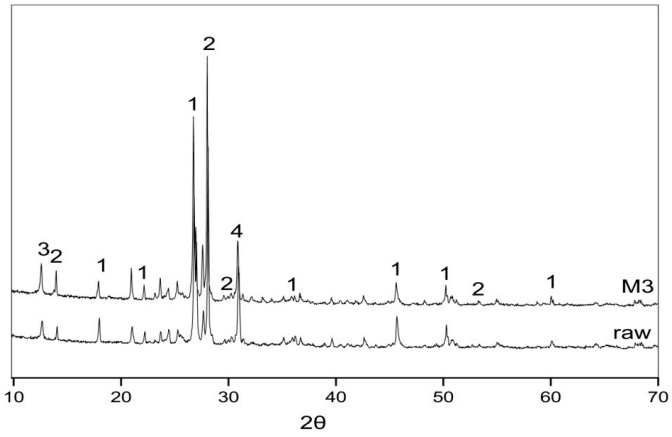

Figure 8. XRD result of raw copper-mine tailings and sample M3 (after 3 h of grinding) (1 quartz, 2 albite, 3 chlorite, 4 dolomite).

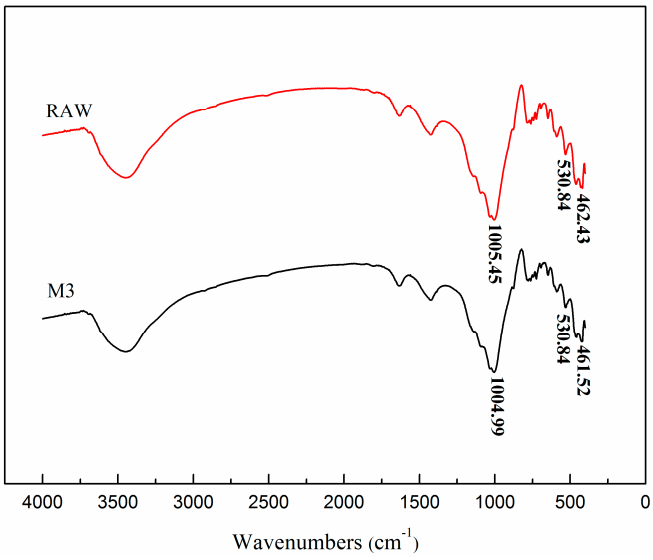

Figure 9. Fourier transform infra-red (FTIR) spectra of raw copper-mine tailings and Sample M3 (after 3 h of grinding).

3.2. Thermal Activation of Copper-Mine Tailings

3.2.1. Thermo-Gravimetric–Differential Scanning Calorimetry (TG–DSC)

Among eight mechanically activated copper-mine tailings, one sample with the maximum leaching concentration of Al and Si was selected and used. The TG–DSC curves of the copper-mine tailings (at the temperature range between 10 °C and 1200 °C under air gas atmosphere) are shown in Figure 10. Based on the results, the weight of copper-mine tailings is slightly reduced at the temperature range of 10–400 °C, which is due to the removal of adsorbed water from copper-mine tailings. A significant decrease in weight was observed at the temperature range of 400–800 °C. In this temperature range, the weight reduction was about 5% and an obvious exothermic peak was observed. In contrast, at 800–1200 °C, no significant change was observed in terms of weight loss. Hence, the thermal activation temperature was set in the range of 400 °C to 800 °C.

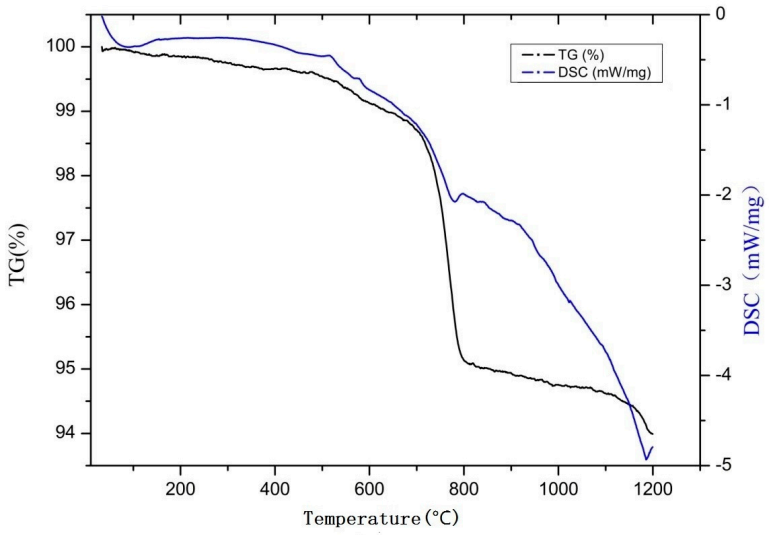

Figure 10. Thermo-gravimetric–differential scanning calorimetry (TG–DSC) curve of raw copper mine tailings (10 °C~1200 °C; atmospheric conditions).

3.2.2. Leaching Test

The experimental results of thermal activation of copper tailings at different temperatures and time intervals are shown in Figure 11. The highest leaching concentrations of Si (57.53 μg/mL) and Al (22.41 μg/mL) are observed at the activation temperature of 600 °C for 120 min. The leaching concentration of raw copper mine tailings is 20.22 μg/mL for Si and 12.22 μg/mL for Al. The percentage increase of Si and Al at the leaching concentration is 54.19% and 119.92%, respectively, after activation. These results are in line with the study of Ahmari et al. [29]. During the thermal-activation process, water evaporation causes the disintegration of the crystal structure and then it repolymerizes, which increases the cementitious activity of Si and Al, and ultimately improves the cementitious activity index of copper-mine tailings. The general mechanism of alumino–silicate cementitious materials is proceeded as (a) dissolution of source material (copper-mine tailings) in the presence of alkaline solution; (b) rearrangement of dissolved ions; (c) hardening of gel-like products (formed due to hydration, i.e., N-A-S-H or C-A-S-H gel) after certain curing conditions (e.g., curing temperature, time, alkali concentration, and water/solid ratio) [30,31].

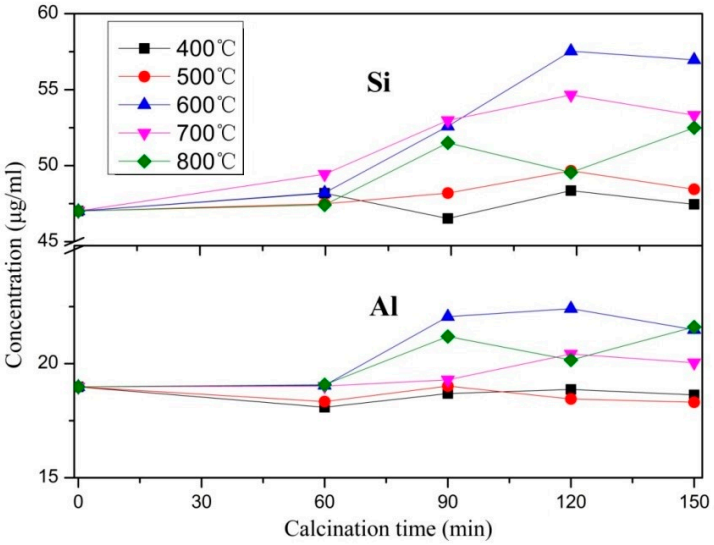

Figure 11. Si and Al concentrations of thermally activated copper tailings after alkali leaching.

3.2.3. Mineral Composition and Particle Morphology

The SEM images of the copper-mine tailings activated at 600 °C for 120 min are shown in Figure 12. It is observed that the particles are irregular in shape and most show a relatively loose and porous surface structure. The thermal activation results in a change in the copper-mine tailings' crystal structures, which can be observed by their fuzzy appearance of edges and corners. In addition, it softens the crystalline structure, which causes better leaching of Si and Al from copper-mine tailings.

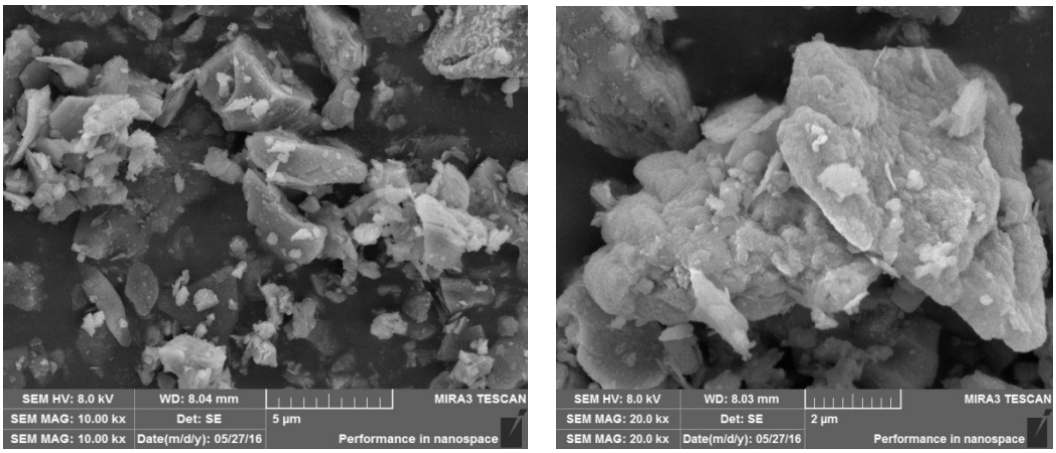

(**a**) 10,000× (**b**) 20,000×

Figure 12. SEM images of the sample TM11 (Table 3) (10,000 (**a**) and 20,000 (**b**) magnification).

Figure 13 shows the XRD patterns of copper-mine tailings activated for 120 min at various temperatures. It can be seen that crystalline chlorite dissolved at 600 °C. This is most likely due to the fact that chlorite crystals are broken down with the increase of temperature. It can be seen from Figure 14 that the Si(Al^{IV})-O-Si asymmetric stretching band of 1004.99 cm^{-1} has disappeared. The Si-O bend vibrations reduced from 530.84 cm^{-1} and 461.52 cm^{-1} to 529.37 cm^{-1} and 460.96 cm^{-1}, respectively. This indicates that the extent of polymerization of $[SiO_4]^{4-}$ and $[AlO_6]^{9-}$ ions is reduced by mechanical grinding. Meanwhile, the Si-O and Si(Al^{IV})-O-Si bonds of copper-mine tailings are broken during thermal activation, which results in a better cementitious activity index of raw copper-mine tailings.

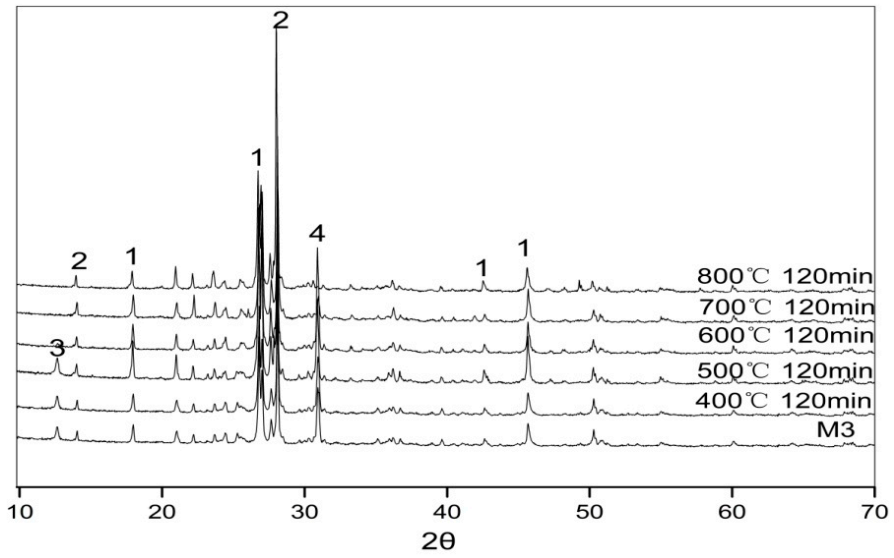

Figure 13. XRD patterns of the thermally activated conditions of copper tailings (1 quartz, 2 albite, 3 chlorite, 4 dolomite).

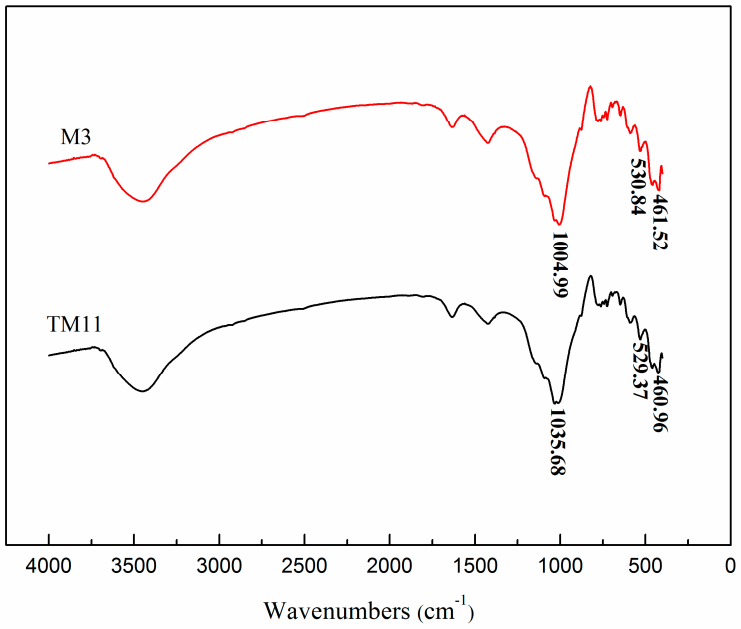

Figure 14. FTIR spectra of the sample M3 (after 3 h of activation, Table 2) and sample TM11 (thermal activation at 600 °C for 120 min, Table 3).

3.3. Alkaline-Roasting Activation of Copper-Mine Tailings

The orthogonal experimental results and range analysis of the Si and Al leaching concentration are shown in Table 7. For the Si leaching concentration, it is shown from the range analysis that the C/N mass ratio(C) is the most important factor and is followed by roasting temperature (B) and roasting time (A). The optimal level of Si is at $A_3B_3C_1$. It can also be seen that the Si leaching concentration increased with roasting time and roasting temperature, and its concentration is decreased as the C/N ratio decreases. On the other hand, the Al leaching concentration is affected in the following order: roasting temperature (B) > roasting time (A) > C/N ratio(C). $A_3B_2C_1$ is the optimal level at which the maximum leaching of Al is noted. It can be observed that the Al leaching concentration increased as the roasting time increased. Moreover, its concentration increased first and then decreased with roasting

temperature. The results indicate that alkaline-roasting activation can greatly improve the activity index of copper-mine tailings. Finally, $A_3B_2C_1$ is the best combination to activate copper-mine tailings. Because, in the case of Si, B3 (Table 7) is the best roasting temperature but there was no significant difference between B2 and B3 (Table 3) and therefore B2 is selected as the best roasting temprature.

Table 7. The orthogonal experimental results and range analysis of Si and Al leaching concentrations.

No.	A (Time)	B (Temp)	C (C/N Mass Ratio)	Si (μg/mL)		Al (μg/mL)
ARMT1	1(60 min)	1(550 °C)	1(5:1)	183.25		62.91
ARMT2	1	2(600 °C)	2(7.5:1)	147.83		48.46
ARMT3	1	3(650 °C)	3(10:1)	159.45		49.55
ARMT4	2(90 min)	1	2	149.23		49.13
ARMT5	2	2	3	150.09		68.19
ARMT6	2	3	1	198.10		79.53
ARMT7	3(120 min)	1	3	151.95		66.35
ARMT8	3	2	1	192.35		88.83
ARMT9	3	3	2	175.92		57.35
	Si			Al		
	A	B	C	A	B	C
kj1	163.51	161.48	191.23	53.64	59.46	70.84
kj2	165.81	163.12	157.66	65.62	68.49	62.14
kj3	173.40	177.82	153.83	70.84	51.65	61.36
R	9.89	16.34	37.40	17.2	16.84	9.48
Order		C > B > A			B > A > C	
Optimal level		A_3, B_3, C_1			A_3, B_2, C_1	

XRD patterns of alkaline roasting-activated copper mine tailings are shown in Figure 15. Crystalline silica and albite exhibit less intensive peaks after activation which indicates that some crystalline silica and albite have been disintegrated, and biotite has been generated; a similar phenomenon has been observed by Ahmari et al. [32]. It can be seen from Figure 16 that the Si(Al^{IV})-O-Si asymmetric stretching band 1033.65 cm^{-1} has disappeared, and 1004.99 cm^{-1} is reduced to 996.51 cm^{-1}. The Si–O bond vibration is reduced from 530.84 cm^{-1} to 529.37 cm^{-1} and 461.52 cm^{-1} to 458.57 cm^{-1}. Wave number 786.93 cm^{-1} represents the [AlO_4] bond vibration and its intensity decreased in alkaline-roasting activation. The O–C–O asymmetric stretching band is observed at 1436.74 cm^{-1}; this may be due to the intensive reaction of NaOH with CO_2 in the presence of air during roasting activation.

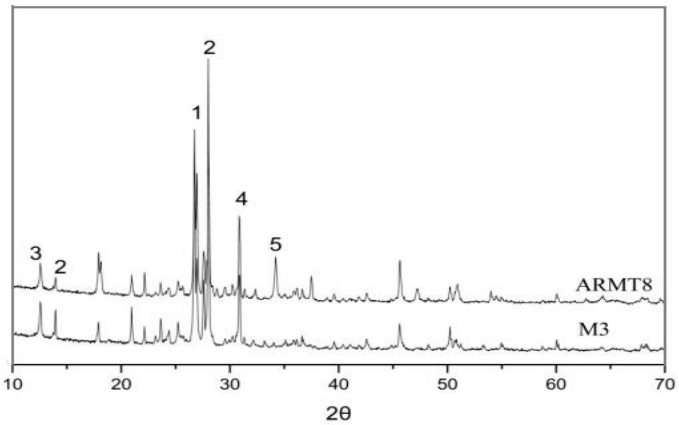

Figure 15. XRD results of the sample M3 (Table 2) and sample ARMT8 (Table 3) (1 quartz, 2 albite, 3 chlorite, 4 dolomite, 5 biotite).

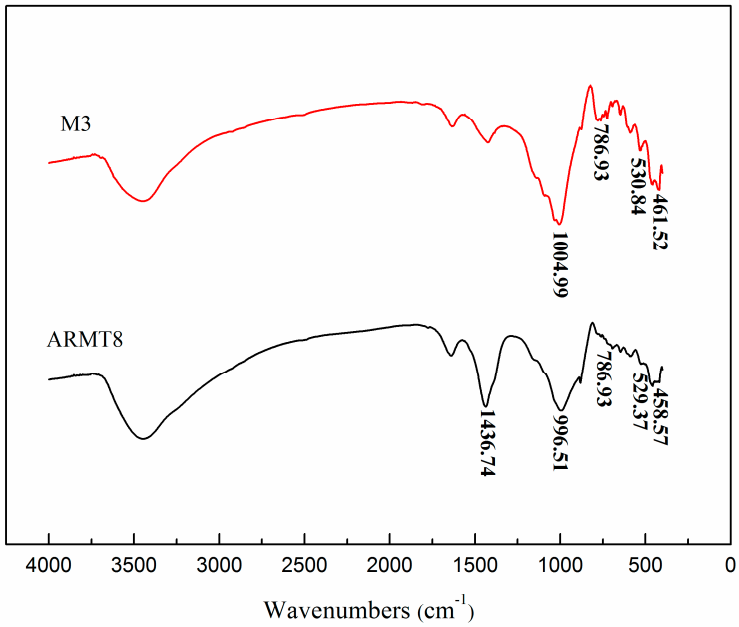

Figure 16. FTIR spectra of the samples M3 (Table 2) (after 3 h of activation) and ARMT8 (Table 3).

4. Conclusions

Based on this study, which investigated the combined approach using mechanical grinding and thermal activation of copper-mine tailings, the following conclusions can be drawn:

(1) In mechanical grinding, activation time is the main factor that significantly affects the cementitious activity of copper-mine tailings. Three hours is the optimal activation time for copper-mine tailings. Increases in leaching concentration of 26.03% (Si) and 93.33% (Al) were observed after activation as compared to raw copper-mine tailings. The particles (D50 and D90) reach their minimum sizes after 3 h of activation.

(2) Activation time and temperature are the two most important factors that affect the thermal activation of copper-mine tailings. Optimal thermal activation conditions are achieved after 120 min at 600 °C. After thermal activation, the percentage increase of Si and Al was 54.19% and 119.92%, respectively.

(3) Alkaline-roasting activation can largely improve the cementitious activity index of copper-mine tailings, and the best results are achieved after 120 min at 600 °C, with a C/N ratio of 5:1.

(4) It is confirmed from SEM images that mechanical grinding and thermal activation change the larger particles into smaller ones, thus increasing the corresponding activity of the particles.

(5) Some of the crystalline silica are broken during mechanical activation, evidenced by less intensive peaks of crystalline silica from the XRD patterns. The Si–O and Si(Al^{IV})–O–Si bonds of copper-mine tailings are supposedly broken during the activation process.

(6) Finally, it is concluded that mechanical, thermal and alkaline-roasting activation significantly influence the dissolution of Al and Si precursors of raw copper-mine tailings. These precursors play a vital role in the cementitious activity of copper-mine tailings. Hence, copper-mine tailings could be utilized in geopolymer systems.

Acknowledgments: This work was supported by the National Natural Science Foundation of China (No. 51404200).

Author Contributions: Lin Yu wrote the main manuscript text. Lin Yu, Zhen Zhang and Xiao Huang participated in the experiments. Binquan Jiao and Dongwei Li supervised the project.

Conflicts of Interest: There are no conflicts of interest to declare.

References

1. Mahasenan, N.; Smith, S.; Humphreys, K. The cement industry and global climate change: Current and potential future cement industry CO_2 emissions. In Proceedings of the 6th International Conference on Greenhouse Gas Control Technologies, Kyoto, Japan, 1–4 October 2002; pp. 995–1000.
2. Gines, O.; Chimenos, J.M.; Vizcarro, A.; Formosa, J.; Rosell, J.R. Combined use of mswi bottom ash and fly ash as aggregate in concrete formulation: Environmental and mechanical considerations. *J. Hazard. Mater.* **2009**, *169*, 643–650. [CrossRef] [PubMed]
3. Mechtcherine, V. Strain-hardening cement-based composites material design, properties and applications in construction. *Beton-Stahlbetonbau* **2015**, *110*, 50–58. [CrossRef]
4. Mohammadinia, A.; Arulrajah, A.; Sanjayan, J.; Disfani, M.M.; Bo, M.W.; Darmawan, S. Laboratory evaluation of the use of cement-treated construction and demolition materials in pavement base and subbase applications. *J. Mater. Civ. Eng.* **2015**, *27*, 04014186. [CrossRef]
5. Wang, A.G.; Deng, M.; Sun, D.S.; Li, B.; Tang, M.S. Effect of crushed air-cooled blast furnace slag on mechanical properties of concrete. *J. Wuhan Univ. Technol.* **2012**, *27*, 758–762. [CrossRef]
6. Qin, W.Z. What role could concrete technology play for sustainability in China? In Proceedings of the International Workshop on Sustainable Development and Concrete Technology, Beijing, China, 20–21 May 2004; pp. 35–43.
7. Pavlik, Z.; Keppert, M.; Pavlikova, M.; Zumar, J.; Fort, J.; Cerny, R. Mechanical, hygric, and durability properties of cement mortar with MSWI bottom ash as partial silica sand replacement. *Cem. Wapno Beton* **2014**, *19*, 67–80.
8. Puertas, F.; Santos, R.; Alonso, M.M.; Del Rio, M. Alkali-activated cement mortars containing recycled clay-based construction and demolition waste. *Ceramics−Silikáty* **2015**, *59*, 202–210.
9. Polozhyi, K.; Reiterman, P.; Keppert, M. Mswi bottom ash as an aggregate for a lightweight concrete. In *Advanced Materials Research*; Trans Tech Publications: Zürich, Switzerland, 2014; Volume 1054, pp. 254–257.
10. Sadi, M.A.K.; Abdullah, A.; Sajoudi, M.N.; Kamal, M.F.B.; Torshizi, F.; Taherkhani, R. Reduce, reuse, recycle and recovery in sustainable construction waste management. In *Advanced Materials Research*; Trans Tech Publications: Zürich, Switzerland, 2012; Volume 446–449, pp. 937–944.
11. Duxson, P.; Provis, J.L.; Lukey, G.C.; Van Deventer, J.S.J. The role of inorganic polymer technology in the development of 'green concrete'. *Cem. Concr. Res.* **2007**, *37*, 1590–1597. [CrossRef]
12. Davidovits, J. Pyramid man-made stone, myth or facts. 3. Cracking the code of the hieroglyphic names of chemicals and minerals involved in the construction. In *Abstracts of Papers of the American Chemical Society*; American Chemical Society: Washington, DC, USA, 1987; Volume 193, p. 37-Hist.
13. Davidovits, J. Geopolymers and geopolymeric materials. *J. Therm. Anal. Calorim.* **1989**, *35*, 429–441. [CrossRef]
14. Davidovits, J. Geopolymers—Inorganic polymeric new materials. *J. Therm. Anal. Calorim.* **1991**, *37*, 1633–1656. [CrossRef]
15. Wastiels, J. Sandwich panels in construction with hpfrcc-faces: New possibilities and adequate modelling. *High Perform. Fiber Reinf. Cem. Compos. (Hpfrcc3)* **1999**, *6*, 143–151.
16. Lofthouse, H. An international journal devoted to innovation and developments in mineral processing and extractive metallurgy. *Min. Eng.* **1999**, *12*, 581–581.
17. Rahier, H.; Wullaert, B.; Van Mele, B. Influence of the degree of dehydroxylation of kaolinite on the properties of aluminosilicate glasses. *J. Therm. Anal. Calorim.* **2000**, *62*, 417–427. [CrossRef]
18. Rahier, H.; VanMele, B.; Wastiels, J. Low-temperature synthesized aluminosilicate glasses. 2. Rheological transformations during low-temperature cure and high-temperature properties of a model compound. *J. Mater. Sci.* **1996**, *31*, 80–85. [CrossRef]
19. Rahier, H.; VanMele, B.; Biesemans, M.; Wastiels, J.; Wu, X. Low-temperature synthesized aluminosilicate glasses. 1. Low-temperature reaction stoichiometry and structure of a model compound. *J. Mater. Sci.* **1996**, *31*, 71–79. [CrossRef]
20. Rahier, H.; Simons, W.; VanMele, B.; Biesemans, M. Low-temperature synthesized aluminosilicate glasses. 3. Influence of the composition of the silicate solution on production, structure and properties. *J. Mater. Sci.* **1997**, *32*, 2237–2247. [CrossRef]

21. Allahverdi, A.; Skvara, F. Sulfuric acid attack on hardened paste of geopolymer cements—Part 2. Corrosion mechanism at mild and relatively low concentrations. *Ceramics−Silikáty* **2006**, *50*, 1–4.
22. Badanoiu, A.; Voicu, G. Influence of raw materials characteristics and processing parameters on the strength of geopolymer cements based on fly ash. *Environ. Eng. Manag. J.* **2011**, *10*, 673–681.
23. Duxson, P.; Provis, J.L. Designing precursors for geopolymer cements. *J. Am. Ceram. Soc.* **2008**, *91*, 3864–3869. [CrossRef]
24. Marin-Lopez, C.; Araiza, J.L.R.; Manzano-Ramirez, A.; Avalos, J.C.R.; Perez-Bueno, J.J.; Muniz-Villareal, M.S.; Ventura-Ramos, E.; Vorobiev, Y. Synthesis and characterization of a concrete based on metakaolin geopolymer. *Inorg. Mater.* **2009**, *45*, 1429–1432. [CrossRef]
25. Zhang, L.Y.; Ahmari, S.; Zhang, J.H. Synthesis and characterization of fly ash modified mine tailings-based geopolymers. *Constr. Build. Mater.* **2011**, *25*, 3773–3781. [CrossRef]
26. Ahmari, S.; Zhang, L.Y.; Zhang, J.H. Effects of activator type/concentration and curing temperature on alkali-activated binder based on copper mine tailings. *J. Mater. Sci.* **2012**, *47*, 5933–5945. [CrossRef]
27. Wang, P.M.; Dong, G.; Chen, Y.M. Ion dissolving-out method on evaluating the pozzolanic activity of coal gangue. In Proceedings of the 6th International Symposium on Cement & Concrete and CANMET/ACI International Symposium on Concrete Technology for Sustainable Development, Xi'an, China, 19–22 September 2006; Volume 2, pp. 1433–1438.
28. Temuujin, J.; Williams, R.P.; van Riessen, A. Effect of mechanical activation of fly ash on the properties of geopolymer cured at ambient temperature. *J. Mater. Process. Technol.* **2009**, *209*, 5276–5280. [CrossRef]
29. Ahmari, S.; Parameswaran, K.; Zhang, L.Y. Alkali activation of copper mine tailings and low-calcium flash-furnace copper smelter slag. *J. Mater. Civ. Eng.* **2015**, *27*, 04014193. [CrossRef]
30. Juenger, M.C.G.; Winnefeld, F.; Provis, J.L.; Ideker, J.H. Advances in alternative cementitious binders. *Cem. Concr. Res.* **2011**, *41*, 1232–1243. [CrossRef]
31. Khale, D.; Chaudhary, R. Mechanism of geopolymerization and factors influencing its development: A review. *J. Mater. Sci.* **2007**, *42*, 729–746. [CrossRef]
32. Ahmari, S.; Zhang, L.Y. Production of eco-friendly bricks from copper mine tailings through geopolymerization. *Constr. Build. Mater.* **2012**, *29*, 323–331. [CrossRef]